

Molecular Structures of Three Diastereoisomers of 3,3'-Di-t-butyl-1,1'-spirobi-indan

Hiroshi Nakai* and Motoo Shiro

Shionogi Research Laboratories, Shionogi and Co. Ltd., Fukushima-ku, Osaka 553, Japan

Seiichi Imajo, Hiroko Kuritani, and Keiji Shingu*

Department of Chemistry, Faculty of Science, Osaka University, Toyonaka, Osaka 560, Japan

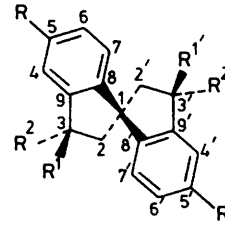
Crystal structures of the three diastereoisomers (+)-(1*R*,3*S*,3'S)-(I), (\pm)-*rel*-(1*R*,3*R*,3'R)-(II), and (\pm)-*rel*-(1*R*,3*R*,3'S)-(III) of the title compound, $C_{25}H_{32}$, have been determined by X-ray analysis. Crystals of (I) are orthorhombic, space group $P2_12_12$, $a = 12.412(1)$, $b = 14.842(1)$, $c = 11.287(1)$ Å, $Z = 4$. Crystals of (II) are monoclinic, space group $P2_1/c$, $a = 16.230(1)$, $b = 11.719(1)$, $c = 11.400(1)$ Å, $\beta = 110.23(1)^\circ$, $Z = 4$. Crystals of (III) are monoclinic, space group $P2_1/c$, $a = 13.220(1)$, $b = 13.877(1)$, $c = 11.897(1)$ Å, $\beta = 109.81(1)^\circ$, $Z = 4$. The structures were solved by the direct method and refined by a block-diagonal least-squares technique to $R = 0.032$ for (I) (1455 reflections), 0.034 for (II) (2146), and 0.044 for (III) (2437). The relative configuration between the chiral centres in each isomer was as expected from ^1H n.m.r. data. The cyclopentene rings are all in envelope conformations, and the tertiary butyl groups adopt quasi-equatorial orientations in agreement with ^1H n.m.r. data except the one in (II), which takes a quasi-axial orientation. The dihedral angles between the two benzene ring planes are 69.5(1), 91.4(1), and 94.9(1) $^\circ$ for (I)—(III), respectively. Calculation for the optimal structure using the MM2 program showed that the discrepancy in the form of (II) can be ascribed to a crystal packing effect.

C.d. spectra of the diastereoisomers of 3,3'-di-t-butyl-1,1'-spirobi-indan, $C_{25}H_{32}$, have been reported to show a noticeable dependence on the conformation caused by puckering of the five-membered rings, even if the configuration at the spiro centre was unchanged.¹ The observed c.d. behaviour was explained on the basis of the mutual arrangement of the two benzene chromophores in each isomer, and an exciton analysis of the interaction between the strong, degenerate 1B transitions was presented.²

The relative configurations and conformations of these isomers were first deduced from n.m.r. data (identification of each diastereotopic methylene proton from the chemical shifts as well as coupling constants with the methine proton), whereupon the configurations at the spiro centre were assigned from the chemically related ones at the 3- and 3'-positions. However, the conformational analyses based on n.m.r. data are often subject to some uncertainty. Accordingly, we undertook crystal structure analyses of the diastereoisomers, (+)-(1*R*,3*S*,3'S)-(I), (\pm)-(1*R*,3*R*,3'R)-(II), and (\pm)-(1*R*,3*R*,3'S)-(III), in order to establish the conformations as well as the relative configurations. The molecular structure of the 3,3,3',3'-tetramethyl derivative of 1,1'-spirobi-indan (IV) in which the spiro atom is the sole chiral centre had been determined by X-ray analysis.³ Thus, comparison between the conformations of these spiro compounds was also expected to give information about the blocking effect of the t-butyl group on the conformational flexibility of the 1,1'-spirobi-indan skeleton.

Experimental

Crystals of (I)—(III) were obtained, respectively, from n-hexane, ethyl acetate—ethanol, and methyl acetate—methanol solutions. Crystallographic details are listed in Table 1. Three-dimensional intensity data were collected on a Hilger and Watts Y 290 diffractometer equipped with a scintillation counter and a pulse-height analyser. Integrated intensities were measured by the θ —2θ scan technique using nickel-filtered $\text{Cu}-K_\alpha$ radiation. Each reflection was integrated in 80 steps at intervals of 0.01° with a measurement time of 1 s per step. Backgrounds were counted for 20 s on both sides of each reflection. One standard



R	R^1	R^2	$R^{1'}$	$R^{2'}$
(I)	H	Bu ^t	H	Bu ^t
(II)	H	H	Bu ^t	H
(III)	H	H	Bu ^t	Bu ^t
(IV)	Me	Me	Me	Me

reflection monitored every 10 reflections showed no significant change during data collection. All intensities were corrected for Lorentz and polarization factors, but not for absorption effects.

Structure Determination and Refinement.—The structures were solved using the direct methods⁴ and improved by block-diagonal least-squares refinement of the positional and the anisotropic thermal parameters of non-hydrogen atoms. Difference electron density maps were calculated, in which all the hydrogen atoms were located. They were given the isotropic temperature factors of the carbon atoms to which they were attached. The thermal parameters of the hydrogen atoms were fixed in the subsequent refinement.

The function minimized in the refinement was $\Sigma(w|\Delta F|^2)$. The weighting scheme is $w = 1/\sigma^2(F_o)$ for observed reflections with $|F_c| \geq \sigma(F_o)$ and $|\Delta F| < 3\sigma(F_o)$, and $w = 0$ otherwise. $\sigma(F_o)$ was estimated as $\sigma(F_o) = [\sigma_1^2(F_o) + c^2|F_o|^2]^{1/2}$, where $\sigma_1(F_o)$ is the standard deviation due to counting errors.⁵ The values of c^2 were respectively 0.00137, 0.00139, and 0.00165 for (I)—(III). The R values ($\Sigma|\Delta F|/\Sigma|F_o|$) converged to 0.032 (for 1455 observed reflections with non-zero weight), 0.034 (2146), and

Table 1. Crystallographic details for (I)–(III)

F.W. Radiation	$C_{25}H_{32}$ 332.5 $Cu-K_\alpha$		
	(I)	(II)	(III)
Crystal system	Orthorhombic	Monoclinic	Monoclinic
Space group	$P2_12_12_1$	$P2_1/c$	$P2_1/c$
$a/\text{\AA}$	12.412(1)	16.230(1)	13.220(1)
$b/\text{\AA}$	14.842(1)	11.719(1)	13.877(1)
$c/\text{\AA}$	11.287(1)	11.400(1)	11.897(1)
$\beta/^\circ$	90.00	110.23(1)	109.81(1)
$U/\text{\AA}^3$	2 079.3(4)	2 034.7(3)	2 053.4(3)
Z	4	4	4
$D_c/\text{g cm}^{-3}$	1.062	1.085	1.076
μ/cm^{-1}	4.5	4.6	4.5
Crystal size/mm	0.3 × 0.4 × 0.4	0.3 × 0.3 × 0.3	0.2 × 0.3 × 0.3
$\theta_{\max.}/^\circ$	57.0	55.0	57.0
Number of unique reflections	1 590	2 551	2 868

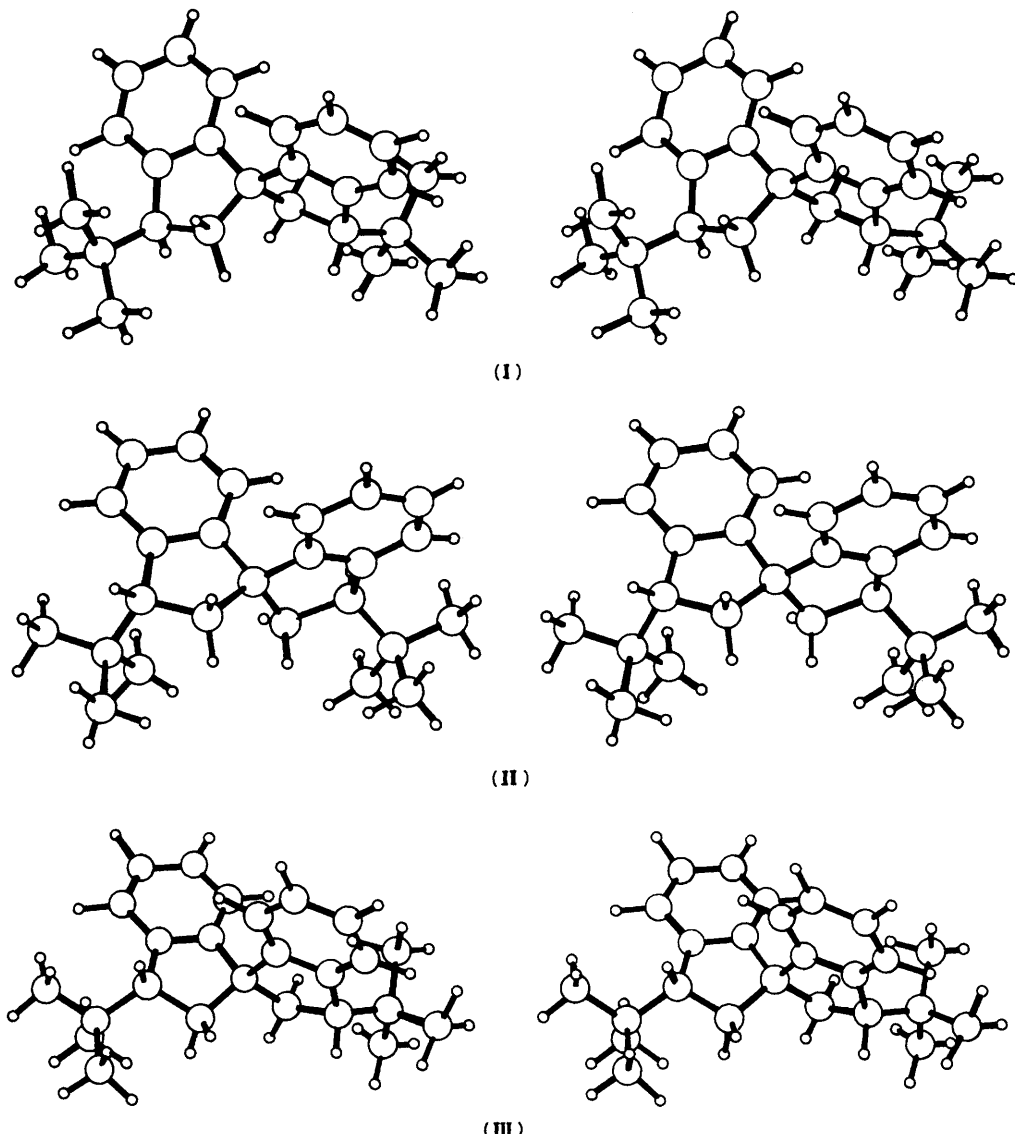
0.044 (2 437) for (I)–(III), respectively. The atomic scattering factors were calculated using the analytical expression $f = \sum [a_i \exp(-b_i \sin^2 \theta / \lambda^2)] + c$ ($i = 1$ –4).⁶ The parameter shifts in the final cycle were less than half the corresponding σ values.

Results and Discussion

The atomic co-ordinates and equivalent isotropic thermal parameters are listed in Table 2,* and PLUTO stereo plottings of the molecules are shown in Figure 1. Each of the relative configurations of the chiral centres corroborated the previous assignment based on ^1H n.m.r. data [*rel*-(1*R*,3*S*,3'*S*), *rel*-(1*R*,3*R*,3'*R*), and *rel*-(1*R*,3*R*,3'*S*) for (I)–(III), respectively].

The benzene rings are nearly planar, but the five-membered rings are puckered almost into the envelope form. The deviations of the flap atoms, C(2) and C(2'), from the best

* Tables of anisotropic thermal parameters are listed in Supplementary Publication No. SUP 56099 (4 pp.). For details see Instructions for Authors, Section 4.0, in *J. Chem. Soc., Perkin Trans. 2*, 1985, Issue 1.

**Figure 1.** PLUTO stereo plottings of the molecules (I)–(III)

planes including four other atoms are particularly large in (I). Torsion angles in the five-membered rings are shown in Table 3. The t-butyl groups all assume quasi-equatorial orientations in agreement with ^1H n.m.r. data except that the one in (II) assumes a quasi-axial orientation. The dihedral angles between

the benzene planes are $69.5(1)$, $91.4(1)$, and $94.9(1)^\circ$ for (I)–(III), respectively, while the corresponding values estimated previously from ^1H n.m.r. data are *ca.* 65 , 105 , and 90° .⁷ It should be noted that the discrepancy between the values for (II) reflects the non- C_2 sense of puckering of the two five-membered rings

Table 2. Atomic co-ordinates ($\times 10^4$, and $\times 10^3$ for hydrogen), and equivalent isotropic temperature factors B_{eq} for carbon and isotropic temperature factors B for hydrogen ($\times 10^2 \text{ \AA}^2$) with their e.s.d.s in parentheses

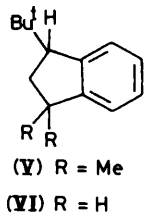
	$B_{\text{eq}} = 4/3 \sum_i \sum_j \beta_{ij} \mathbf{a}_i \cdot \mathbf{a}_j$					B_{eq}/B			
	x	y	z	B_{eq}/B		x	y	z	B_{eq}/B
(I)									
C(1)	1 916(1)	2 650(1)	4 413(1)	382(4)	H(C5)	-55(1)	229(1)	64(1)	498
C(2)	2 668(1)	1 848(1)	4 133(1)	427(4)	H(C6)	-114(1)	319(1)	216(1)	479
C(3)	2 654(1)	1 737(1)	2 775(2)	425(4)	H(C7)	-12(1)	337(1)	414(1)	446
C(4)	923(2)	1 996(1)	1 448(2)	525(5)	H(C11)	209(1)	5(1)	331(1)	500
C(5)	-76(2)	2 397(1)	1 378(2)	565(5)	H'(C11)	143(1)	22(1)	197(1)	500
C(6)	-477(1)	2 893(1)	2 301(2)	540(5)	H''(C11)	234(1)	-60(1)	217(1)	500
C(7)	123(1)	2 999(1)	3 337(2)	464(4)	H(C12)	373(1)	141(1)	60(1)	550
C(8)	1 115(1)	2 584(1)	3 407(1)	389(3)	H'(C12)	348(1)	25(1)	53(1)	550
C(9)	1 524(1)	2 077(1)	2 477(1)	404(4)	H''(C12)	248(1)	80(1)	51(1)	550
C(10)	3 010(1)	797(1)	2 323(2)	525(5)	H(C13)	460(1)	93(1)	294(1)	530
C(11)	2 140(2)	83(1)	2 514(2)	656(6)	H'(C13)	408(1)	61(1)	373(1)	530
C(12)	3 286(2)	850(2)	999(2)	767(7)	H''(C13)	426(1)	-9(1)	263(1)	530
C(13)	4 032(2)	522(2)	2 971(3)	689(6)	H(C2')	320(1)	364(1)	385(1)	427
C(2')	2 520(1)	3 559(1)	4 432(1)	408(4)	H'(C2')	198(1)	404(1)	430(1)	427
C(3')	2 913(1)	3 696(1)	5 711(1)	393(3)	H(C3')	370(1)	332(1)	579(1)	447
C(4')	1 868(2)	3 147(1)	7 622(1)	486(4)	H(C4')	235(1)	358(1)	824(1)	463
C(5')	1 063(2)	2 586(1)	8 056(2)	546(5)	H(C5')	96(1)	257(1)	896(1)	496
C(6')	468(1)	2 039(1)	7 305(2)	522(5)	H(C6')	-4(1)	157(1)	756(1)	454
C(7')	694(2)	2 036(1)	6 101(2)	471(4)	H(C7')	18(1)	170(1)	538(1)	480
C(8')	1 492(1)	2 602(1)	5 674(1)	382(4)	H(C11')	233(1)	576(1)	650(1)	525
C(9')	2 072(1)	3 172(1)	6 419(1)	390(3)	H'(C11')	173(1)	523(1)	542(1)	525
C(10')	3 143(1)	4 693(1)	6 048(2)	453(4)	H''(C11')	149(1)	494(1)	684(1)	525
C(11')	2 100(2)	5 223(1)	6 194(2)	629(6)	H(C12')	430(1)	435(1)	719(1)	501
C(12')	3 778(2)	4 735(2)	7 212(2)	646(6)	H'(C12')	400(1)	543(1)	732(1)	501
C(13')	3 827(2)	5 127(1)	5 083(2)	600(5)	H''(C12')	324(1)	446(1)	803(1)	501
H(C2)	343(1)	198(1)	444(1)	446	H(C13')	346(1)	509(1)	424(1)	500
H'(C2)	236(1)	118(1)	454(1)	446	H'(C13')	400(1)	588(1)	537(1)	500
H(C3)	317(1)	220(1)	247(1)	434	H''(C13')	461(1)	473(1)	508(1)	500
H(C4)	123(1)	153(1)	74(1)	479					
(II)									
C(1)	7 774(1)	4 618(1)	5 686(1)	319(3)	H(C5)	1 027(1)	223(1)	887(1)	452
C(2)	7 243(1)	3 586(1)	4 952(1)	368(3)	H(C6)	1 016(1)	417(1)	930(1)	450
C(3)	7 849(1)	2 532(1)	5 240(1)	340(3)	H(C7)	906(1)	536(1)	796(1)	386
C(4)	9 225(1)	2 214(1)	7 290(1)	430(4)	H(C11)	612(1)	196(1)	390(1)	550
C(5)	9 812(1)	2 707(1)	8 359(1)	467(4)	H'(C11)	681(1)	138(1)	326(1)	550
C(6)	9 749(1)	3 844(1)	8 598(1)	461(4)	H''(C11)	627(1)	56(1)	383(1)	550
C(7)	9 101(1)	4 516(1)	7 779(1)	401(4)	H(C12)	758(1)	-30(1)	507(1)	546
C(8)	8 501(1)	4 020(1)	6 722(1)	330(3)	H'(C12)	829(1)	49(1)	461(1)	546
C(9)	8 555(1)	2 871(1)	6 472(1)	333(3)	H''(C12)	845(1)	33(1)	615(1)	546
C(10)	7 355(1)	1 393(1)	5 187(1)	387(3)	H(C13)	666(1)	54(1)	613(1)	532
C(11)	6 583(1)	1 346(1)	3 949(1)	586(5)	H'(C13)	752(1)	128(1)	705(1)	532
C(12)	7 952(1)	372(1)	5 217(2)	556(5)	H''(C13)	658(1)	193(1)	622(1)	532
C(13)	7 010(1)	1 281(1)	6 267(1)	532(5)	H(C2')	663(1)	512(1)	606(1)	387
C(2')	7 225(1)	5 488(1)	6 136(1)	385(4)	H'(C2')	758(1)	572(1)	696(1)	387
C(3')	7 048(1)	6 559(1)	5 274(1)	361(3)	H(C3')	717(1)	725(1)	585(1)	358
C(4')	8 002(1)	7 221(1)	3 950(1)	415(4)	H(C4')	778(1)	807(1)	388(1)	417
C(5')	8 637(1)	6 923(1)	3 449(1)	438(4)	H(C5')	881(1)	748(1)	290(1)	443
C(6')	9 022(1)	5 858(1)	3 667(1)	405(3)	H(C6')	946(1)	565(1)	332(1)	404
C(7')	8 778(1)	5 075(1)	4 395(1)	366(3)	H(C7')	906(1)	433(1)	462(1)	361
C(8')	8 128(1)	5 362(1)	4 874(1)	307(3)	H(C11')	548(1)	595(1)	542(1)	681
C(9')	7 734(1)	6 426(1)	4 653(1)	333(3)	H'(C11')	573(1)	750(1)	571(1)	681
C(10')	6 084(1)	6 707(1)	4 371(1)	439(4)	H''(C11')	487(1)	668(1)	460(1)	681
C(11')	5 476(1)	6 773(2)	5 144(2)	730(6)	H(C12')	531(1)	798(1)	323(1)	635
C(12')	5 985(1)	7 846(1)	3 672(2)	677(6)	H'(C12')	621(1)	844(1)	440(1)	635
C(13')	5 802(1)	5 739(1)	3 436(2)	650(5)	H''(C12')	629(1)	781(1)	298(1)	635
H(C2)	675(1)	342(1)	522(1)	372	H(C13')	516(1)	594(1)	276(1)	645
H'(C2)	704(1)	372(1)	404(1)	372	H'(C13')	617(1)	585(1)	299(1)	645
H(C3)	813(1)	242(1)	462(1)	327	H''(C13')	571(1)	511(1)	386(1)	645
H(C4)	930(1)	141(1)	707(1)	415					

Table 2 (continued)

	$B_{eq} = 4/3 \sum_i \sum_j \beta_{ij} \mathbf{a}_i \cdot \mathbf{a}_j$					$B_{eq} = 4/3 \sum_i \sum_j \beta_{ij} \mathbf{a}_i \cdot \mathbf{a}_j$			
	x	y	z	B_{eq}/B	x	y	z	B_{eq}/B	
(III)									
C(1)	6.821(1)	2.023(1)	1.487(1)	402(4)	H(C5)	526(1)	518(1)	288(1)	550
C(2)	5.747(1)	1.635(1)	618(2)	455(5)	H(C6)	723(1)	505(1)	322(1)	508
C(3)	4.833(1)	2.109(1)	950(1)	382(4)	H(C7)	800(1)	370(1)	267(1)	457
C(4)	4.916(1)	3.858(1)	1.861(2)	494(5)	H(C11)	351(1)	67(1)	2(1)	541
C(5)	5.581(2)	4.607(1)	2.440(2)	593(6)	H'(C11)	404(1)	100(1)	-122(1)	541
C(6)	6.677(2)	4.549(1)	2.721(2)	572(6)	H'(C11)	272(1)	122(1)	-140(1)	541
C(7)	7.138(1)	3.734(1)	2.433(2)	498(5)	H(C12)	292(1)	303(1)	74(1)	533
C(8)	6.477(1)	2.987(1)	1.839(1)	394(4)	H'(C12)	283(1)	192(1)	105(1)	533
C(9)	5.370(1)	3.036(1)	1.547(1)	376(4)	H'(C12)	210(1)	232(1)	-34(1)	533
C(10)	3.749(1)	2.181(1)	-95(1)	428(4)	H(C13)	303(1)	292(1)	-172(1)	552
C(11)	3.488(1)	1.200(1)	-719(2)	579(6)	H'(C13)	446(1)	269(1)	-136(1)	552
C(12)	2.843(1)	2.405(2)	397(2)	601(6)	H'(C13)	395(1)	360(1)	-53(1)	552
C(13)	3.784(2)	2.938(1)	-1.006(2)	608(6)	H(C2')	737(1)	219(1)	0(1)	465
C(2')	7.721(1)	2.067(1)	930(2)	531(5)	H'(C2')	819(1)	269(1)	124(1)	465
C(3')	8.481(1)	1.213(1)	1.395(2)	515(5)	H(C3')	823(1)	68(1)	74(1)	477
C(4')	8.721(2)	2.08(1)	3.353(2)	654(6)	H(C4')	951(1)	-13(1)	334(1)	589
C(5')	8.323(2)	30(1)	4.274(2)	721(7)	H(C5')	875(1)	-50(1)	501(1)	597
C(6')	7.436(2)	513(1)	4.353(2)	644(6)	H(C6')	713(1)	34(1)	513(1)	582
C(7')	6.921(1)	1.187(1)	3.479(2)	511(5)	H(C7')	628(1)	160(1)	355(1)	487
C(8')	7.312(1)	1.365(1)	2.555(1)	417(4)	H(C11')	929(1)	136(1)	-31(1)	709
C(9')	8.225(1)	895(1)	2.490(2)	483(5)	H'(C11')	1.037(1)	193(1)	49(1)	709
C(10')	9.664(1)	1.449(2)	1.544(2)	746(7)	H''(C11')	939(1)	252(1)	32(1)	709
C(11')	9.696(2)	1.884(2)	386(2)	917(9)	H(C12')	1.117(1)	91(1)	171(1)	868
C(12')	10.346(2)	528(3)	1.788(3)	1.281(13)	H'(C12')	980(1)	8(1)	108(1)	868
C(13')	10.141(2)	2.162(3)	2.573(3)	1.110(12)	H''(C12')	1.073(1)	43(1)	276(1)	868
H(C2)	556(1)	179(1)	-38(1)	450	H(C13')	1.006(1)	165(1)	343(1)	830
H'(C2)	570(1)	92(1)	61(1)	450	H'(C13')	948(1)	285(1)	233(1)	830
H(C3)	461(1)	170(1)	160(1)	371	H''(C13')	1.086(1)	225(1)	270(1)	830
H(C4)	407(1)	400(1)	155(1)	505					

Table 3. Torsion angles ($^{\circ}$) in the five-membered ring and the dihedral angle of the t-butyl group with respect to the benzene ring, with e.s.d.s in parentheses. Values for primed atoms follow those for unprimed atoms

	(I)	(II)	(III)
C(8)-C(1)-C(2)-C(3)	30.1(2)	29.4(1)	-22.0(2)
C(2)-C(1)-C(8)-C(9)	-19.2(2)	-20.0(2)	14.6(2)
C(1)-C(2)-C(3)-C(9)	-29.8(2)	-28.0(1)	-21.3(2)
C(2)-C(3)-C(9)-C(8)	18.2(2)	15.8(2)	-12.3(2)
C(1)-C(8)-C(9)-C(3)	0.6(2)	2.8(2)	-1.6(2)
C(10)-C(3)-C(9)-C(4)	-38.9(3)	-41.6(3)	45.3(2)
		66.3(2)	64.3(2)
			-47.9(4)



in the crystalline state, which is similar to (III) with regard to the spirobi-indan skeleton.

Bond lengths and angles involving only heavy atoms are given in Table 4. The spiro angles C(2)-C(1)-C(8) and C(2')-C(1)-C(8') are almost the same, but as for the other bond angles around C(1), C(8)-C(1)-C(8') in (I) and C(8)-C(1)-C(2') in (II) and (III) are relatively large. These are probably due to the steric repulsion between H[C(7)] and C(8'), and H[C(7')] and C(8) in (I) and between H[C(7)] and H'[C(2')] in (II) and (III), which originally results from the puckering of the five-membered rings in each isomer. The repulsion between the t-butyl group and the adjacent benzene ring is reduced by the increase of the angle C(9)-C(3)-C(10), and moreover, by the bending and torsion of the connection between the benzene and C(1)-C(3)-C(8)-C(9) planes, which are reflected, respectively,

by the differences between the deviations of C(2) atom from the individual planes, and between the deviations of C(1) and C(3) atoms from the benzene plane (Table 5). The only exception is found in one indan unit of (II), in which the t-butyl group assumes a quasi-axial orientation as described above.

Calculation for the optimal structure using the MM2 program⁸ showed that, in 1,1'-dimethyl-3-t-butylindan (V), the quasi-equatorial conformer (conformer with the t-butyl group quasi-equatorial; the deviation of the flap atom $d = 0.45 \text{ \AA}$) was more stable by 5.9 kJ mol^{-1} than the quasi-axial one ($d = 0.18 \text{ \AA}$), as opposed to 1-t-butylindan (VI), in which the quasi-axial conformer ($d = 0.43 \text{ \AA}$) was more stable by 3.3 kJ mol^{-1} than the quasi-equatorial one ($d = 0.47 \text{ \AA}$). This shows that, in (V), the 1,3-interaction between the t-butyl group and the confronting substituent outweighs the repulsion between the former and the adjacent benzene ring, thus favouring the quasi-equatorial conformer. The ^1H n.m.r. data of (V) and (VI) supported the calculation results.* Similarly, the spiro com-

* ^1H N.m.r. data (CDCl_3) for methine (H_x) and adjacent methylene protons (H_A ; *trans* to H_x , H_B ; *cis* to H_x) for (V) (100 MHz) and (VI) (360 MHz) were as follows: (V) H_A δ 1.67, H_B 1.92, H_x 3.13 (J_{AB} 12.5, J_{AX} 10.7, J_{BX} 7.3 Hz); (VI) H_A δ 2.02, H_B 2.12, H_x 2.95 (J_{AB} 13.2, J_{AX} 3.8, J_{BX} 8.7 Hz).

Table 4. Bond lengths (\AA) and angles ($^\circ$), with their e.s.d.s in parentheses. Values for primed atoms follow those for unprimed atoms

	(I)		(II)		(III)	
C(1)–C(2)	1.545(2)	1.544(2)	1.551(2)	1.553(2)	1.543(3)	1.547(3)
C(1)–C(8)	1.512(2)	1.519(2)	1.521(2)	1.522(2)	1.517(2)	1.520(2)
C(2)–C(3)	1.542(3)	1.537(2)	1.542(2)	1.558(2)	1.540(3)	1.531(3)
C(3)–C(9)	1.528(3)	1.527(2)	1.527(2)	1.520(2)	1.524(2)	1.518(3)
C(3)–C(10)	1.550(3)	1.554(3)	1.547(2)	1.557(2)	1.550(2)	1.548(4)
C(4)–C(5)	1.378(4)	1.390(4)	1.387(2)	1.385(2)	1.385(4)	1.389(4)
C(4)–C(9)	1.386(3)	1.382(3)	1.394(2)	1.393(2)	1.397(3)	1.392(4)
C(5)–C(6)	1.369(3)	1.387(3)	1.371(2)	1.379(2)	1.375(4)	1.381(4)
C(6)–C(7)	1.395(3)	1.388(3)	1.385(2)	1.384(2)	1.382(4)	1.393(4)
C(7)–C(8)	1.379(3)	1.385(3)	1.388(2)	1.387(2)	1.385(3)	1.386(3)
C(8)–C(9)	1.388(2)	1.393(2)	1.385(2)	1.384(2)	1.387(2)	1.397(3)
C(10)–C(11)	1.528(3)	1.524(3)	1.530(2)	1.535(3)	1.533(3)	1.518(4)
C(10)–C(12)	1.535(4)	1.533(4)	1.533(3)	1.534(3)	1.533(3)	1.534(5)
C(10)–C(13)	1.520(4)	1.524(3)	1.524(2)	1.515(3)	1.521(3)	1.534(5)
C(2)–C(1)–C(2')	112.5(1)		114.5(1)		113.2(2)	
C(2)–C(1)–C(8')	111.4(1)		112.0(1)		112.7(1)	
C(8)–C(1)–C(2')	112.7(1)		115.2(1)		115.4(1)	
C(8)–C(1)–C(8')	118.2(1)		112.4(1)		112.5(1)	
C(2)–C(1)–C(8)	101.2(1)	101.3(1)	101.3(1)	101.8(1)	101.5(1)	102.1(1)
C(1)–C(2)–C(3)	106.2(1)	106.4(1)	108.4(1)	108.8(1)	107.6(2)	108.7(2)
C(2)–C(3)–C(9)	101.2(2)	102.0(1)	102.0(1)	101.9(1)	101.4(1)	103.0(2)
C(2)–C(3)–C(10)	114.9(2)	114.5(1)	113.5(1)	115.5(1)	114.5(1)	113.0(2)
C(9)–C(3)–C(10)	119.1(2)	118.8(1)	118.3(1)	115.7(1)	118.5(1)	118.3(2)
C(5)–C(4)–C(9)	119.7(2)	119.6(2)	119.8(1)	119.6(1)	119.2(2)	119.6(2)
C(4)–C(5)–C(6)	121.0(2)	121.2(2)	120.2(2)	120.6(2)	121.1(2)	121.6(2)
C(5)–C(6)–C(7)	120.3(2)	119.5(5)	120.7(2)	120.2(2)	120.3(2)	119.1(2)
C(6)–C(7)–C(8)	118.3(2)	118.9(2)	119.2(1)	119.3(1)	118.9(2)	119.5(2)
C(1)–C(8)–C(7)	126.9(2)	127.0(2)	127.2(1)	126.8(1)	127.2(1)	127.0(1)
C(1)–C(8)–C(9)	111.3(1)	111.0(1)	112.0(1)	112.3(1)	111.3(1)	111.5(1)
C(7)–C(8)–C(9)	121.7(2)	121.9(2)	120.7(2)	120.9(2)	121.4(2)	121.5(2)
C(3)–C(9)–C(4)	130.5(2)	130.8(2)	129.4(1)	128.6(1)	129.7(1)	130.2(2)
C(3)–C(9)–C(8)	110.4(1)	110.3(1)	111.2(1)	112.0(1)	111.2(1)	111.1(2)
C(4)–C(9)–C(8)	119.0(2)	118.8(2)	119.3(1)	119.4(1)	119.0(1)	118.6(2)
C(3)–C(10)–C(11)	112.1(2)	111.2(2)	108.4(1)	108.9(1)	109.1(1)	108.5(2)
C(3)–C(10)–C(12)	109.8(2)	110.0(2)	110.9(1)	109.9(1)	109.7(1)	110.6(2)
C(3)–C(10)–C(13)	108.7(2)	109.3(2)	111.9(1)	111.8(1)	111.9(1)	110.7(2)
C(11)–C(10)–C(12)	109.3(2)	108.8(2)	107.6(1)	106.4(2)	106.8(2)	107.9(3)
C(11)–C(10)–C(13)	109.6(2)	109.4(2)	109.2(1)	110.1(2)	108.9(2)	109.7(3)
C(12)–C(10)–C(13)	107.2(2)	108.0(2)	108.7(1)	109.5(2)	110.4(2)	109.3(3)

Table 5. Deviations (\AA) of the atoms from the least-squares plane, with e.s.d.s in parentheses. Values for primed atoms followed those for unprimed atoms

Plane: C(1), C(3), C(8), C(9)

	(I)		(II)		(III)	
C(1)	0.002(1)	0.008(1)	0.005(2)	0.001(2)	0.002(1)	-0.003(1)
C(3)	-0.004(2)	-0.008(1)	-0.004(2)	-0.001(2)	-0.002(1)	0.010(2)
C(8)	-0.003(1)	-0.015(1)	-0.008(2)	-0.002(2)	-0.003(1)	0.006(1)
C(9)	0.003(1)	0.015(1)	0.008(2)	0.002(2)	0.003(1)	-0.018(2)
C(2)	-0.487(1)	-0.464(1)	-0.352(2)	0.285(2)	-0.411(2)	0.305(2)

Plane: C(4)–C(9)

C(4)	0.012(2)	-0.018(2)	0.011(2)	0.013(2)	0.007(2)	-0.008(3)
C(5)	-0.004(2)	-0.006(2)	-0.005(2)	-0.004(2)	-0.003(3)	-0.006(3)
C(6)	-0.005(2)	0.015(2)	-0.006(2)	-0.007(2)	-0.006(3)	0.008(3)
C(7)	0.006(2)	-0.005(2)	0.010(2)	0.011(2)	0.007(2)	0.003(2)
C(8)	0.001(1)	-0.007(1)	-0.003(2)	-0.003(2)	-0.001(1)	-0.005(1)
C(9)	-0.004(1)	0.011(1)	-0.008(2)	-0.009(2)	-0.001(1)	0.016(2)
C(1)	0.083(1)	-0.130(1)	0.077(2)	0.011(2)	0.065(1)	-0.097(1)
C(2)	-0.374(1)	0.336(1)	-0.263(2)	0.288(2)	-0.318(2)	0.211(2)
C(3)	0.059(2)	-0.032(1)	0.030(2)	-0.011(2)	0.052(1)	-0.004(2)

pound (I)–(III) were found to be most stable in their respective di-quasi-equatorial conformations [(I)-1, (II)-1, and (III)-1, as shown in Figure 2] and their calculated dihedral

angles between the benzene planes (67, 101, 93°, respectively) agreed fairly well with the ^1H n.m.r. data.

However, (II) and (III) were found to assume metastable

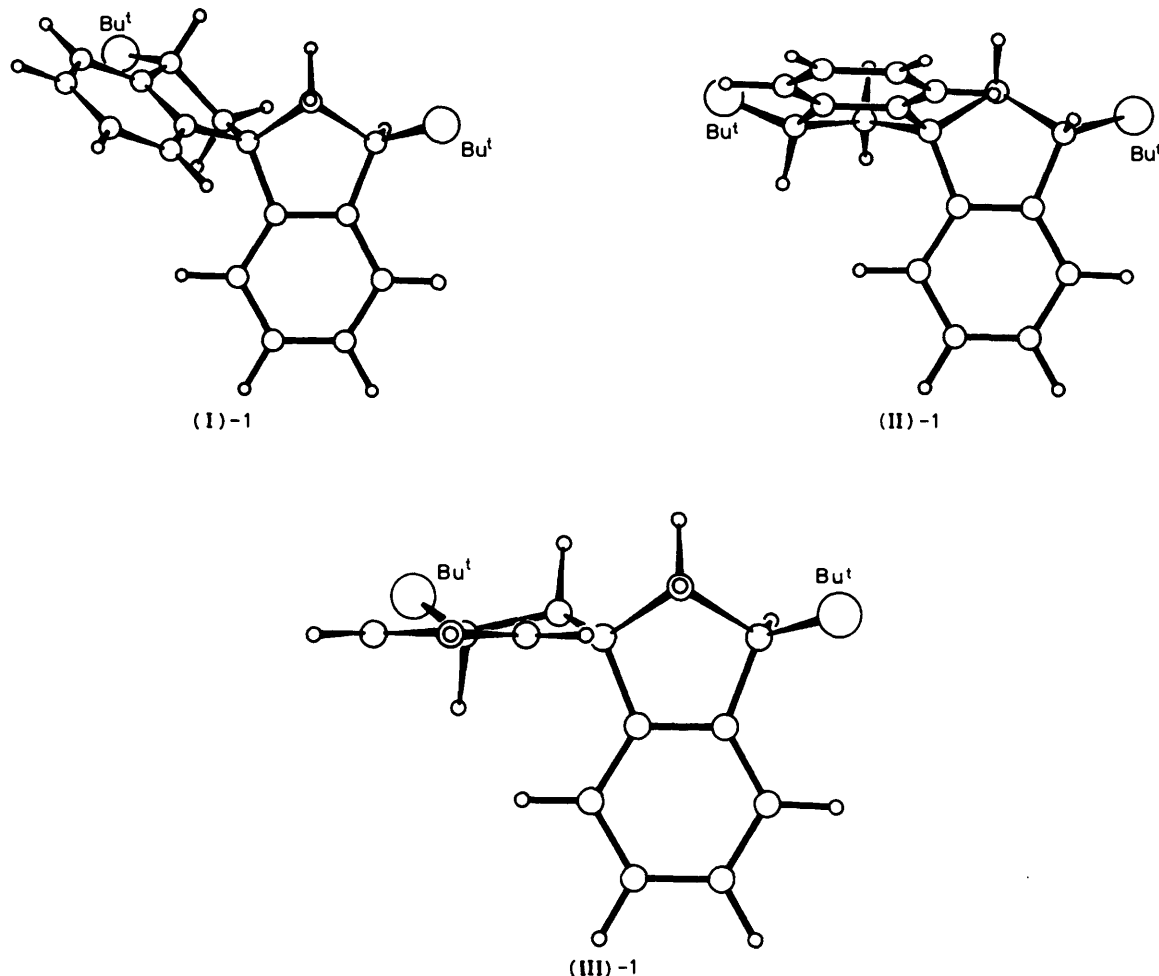


Figure 2. Schematic views of the most stable conformers, (I)-1, (II)-1, and (III)-1. One of the benzene rings in each isomer was placed on the plane of the paper

forms [(II)-2 and (III)-2; quasi-axial in one *cis*-indan unit*] which are less stable by 2.5 and 2.9 kJ mol⁻¹, respectively, than (II)-1 and (III)-1, and the di-quasi-axial conformer (II)-3 was more unstable by 6.3 kJ mol⁻¹ than (II)-1. These rather small energy differences can be ascribed to the lower stabilities of (II)-1 and (III)-1 [by 3.7 and 3.2 kJ mol⁻¹ than (I)-1], which originate from the close proximity of H[C(3)] to H[C(7)] {and H[C(3')] to H[C(7)]} in (II)-1 and H'[C(2')] to H[C(7)] in (III)-1, respectively. It was also shown that the *trans*-indan unit* could not assume the quasi-axial form owing to a large steric repulsion between the t-butyl group and the confronting benzene ring, and that the metastable form of this unit was nearly planar [(I)-2 and (III)-3; quasi-equatorial and quasi-axial in another unit of each, and less stable by 9.6 and 9.2 kJ mol⁻¹ than (I)-1 and (III)-2, respectively].

Thus, the molecular conformations found for (I) and (III) by X-ray analyses agree well with the calculation, and the conformational reversal observed for (II) might be ascribed to some

crystal packing force which overwhelms the small difference in conformational energy.

References

- 1 S. Imajo, A. Kato, and K. Shingu, *J. Chem. Soc., Chem. Commun.*, (a) 1978, 810; (b) 1979, 25.
 - 2 K. Shingu, S. Imajo, H. Kuritani, S. Hagishita, and K. Kuriyama, *J. Am. Chem. Soc.*, 1983, **105**, 6966.
 - 3 M. Shiro, S. Hagishita, and K. Kuriyama, *J. Chem. Soc., Perkin Trans. 2*, 1976, 1447.
 - 4 P. Main, S. E. Hull, L. Lessinger, G. Germain, J. P. Declercq, and M. M. Woolfson, 'MULTAN 78: A System of Computer Programs for the Automatic Solution of Crystal Structures from X-Ray Diffraction Data,' Universities of York, and Louvain.
 - 5 D. F. Grant, R. C. G. Killean, and J. L. Lawrence, *Acta Crystallogr.*, 1969, **B25**, 347.
 - 6 'International Tables for X-Ray Crystallography,' Kynoch Press, Birmingham, 1974, vol. IV.
 - 7 S. Imajo, A. Kato, K. Shingu, and H. Kuritani, *Tetrahedron Lett.*, 1981, **22**, 2179.
 - 8 N. L. Allinger and Y. H. Yuh, MM2: QCPE program No. 395, Quantum Chemistry Program Exchange, University of Indiana.

* We call the indan unit, which has the t-butyl group at the *cis* or *trans* position to the confronting methylene group, *cis* or *trans*, respectively.

Received 3rd January 1984; Paper 4/008